Investigation of pressure distribution in an Archimedes Screw Turbine with head below one meter using CFD

MI. Maulana[1*], Ratna Sary[1], A. Syuhada[1], Siska Mayasari[1], Yusmanizar[2]

[1]Program Studi Teknik Mesin Jurusan Teknik Mesin dan Industri, Universitas Syiah Kuala, Banda Aceh, 23111, Indonesia

[2]Program Studi Teknik Pertanian, Universitas Syiah Kuala, Banda Aceh, 23111, Indonesia

*Corresponding author: ilhammaulana@usk.ac.id

Abstract

In the shift from fossil fuel-based energy, the imperative of tapping into water resources as a renewable energy reservoir is underscored. This study delves into the potential of low-head water for small-scale power generation, specifically focusing on the Archimedes turbine designed for operation in such conditions. The primary objective is meticulously examining pressure characteristics at varying heads (0.7 m, 0.8 m, 0.9 m, and 1 m) using Computational Fluid Dynamics (CFD). These parameters play a crucial role in defining the turbine's performance landscape. Data analysis reveals a notable reduction in the Archimedes turbine's efficiency as the head diminishes. Interestingly, the double-screw Archimedes turbine demonstrates optimal performance at higher flow rates, particularly at a volumetric flow rate of 0.025 m^3/s. Despite the peak performance at a 1-meter head, pressure patterns suggest sufficient kinetic energy within lower head flows (down to 0.7 meters) to facilitate turbine rotation. This study contributes to a more rigorous understanding of the Archimedes turbine's performance under varied head conditions, emphasizing the potential for practical power generation at lower head levels.

Keywords:

Renewable energy, Archimedes, Computational Fluid Dynamics (CFD), turbine head, performance.

1 Introduction

Hydroelectric power is a pivotal energy source in Indonesia's pursuit of Sustainable Development Goal 7—achieving widespread use of renewable energy[1], [2]. This commitment is evident in Indonesia's remarkable electrification ratio of 99.20%, with a specific focus on harnessing micro-hydro energy to address the energy needs of remote and inaccessible areas[1], [3], [4]. The Micro Hydro Power Plant (PLTMH) is a viable alternative for supplying electricity to challenging terrains. Notably, Aceh, which is characterized by relatively low flow potential, strategically employs the Archimedes Screw Turbine (AST) due to its suitability for low water potential applications[5],[6].

The AST presents several advantages, including its ability to operate at low heads, ease of installation and maintenance, minimal disruption to river ecology, and fish-friendly characteristics[7], [8]. By converting water's kinetic and potential energy into electricity, the AST proves to be an efficient and environmentally friendly energy solution[9].

Past research efforts, both experimental and numerical, have been dedicated to optimizing AST designs[10]. Researchers have explored parameters such as runner blade configuration[11], [12], inlet flow conditions[13], [14], turbine slope[15], and various combinations thereof to obtain optimal turbine designs[16]–[18] and turbine performance [16], [19], [20]. Despite the advantages of experimental research, the significant time and cost have prompted researchers to turn to numerical simulations. This approach allows for a cost-effective and time-efficient exploration of flow characteristic values within the turbine, complementing findings that may be challenging to measure experimentally[21]–[24].

However, a notable gap in existing research pertains to the performance of low-head Archimedes turbines below 1 meter despite the prevalence of such conditions in numerous rivers and irrigation systems in Indonesia. This research addresses this gap by conducting simulations to assess the impact of head variations (0.7 m, 0.8 m, 0.9 m, and 1 m) on heat and pressure within the turbine, providing valuable insights into the dynamics of low-head Archimedes turbines.

2 Research Methods

The method used in this research is numerical simulation of an Archimedes turbine, which has dimensions as shown in Fig. 1 and Table 1.

Table 1. Table 1 Design parameters of the Archimedes turbine

Parameters	Dimension (m)
Head (H)	0.7
	0.8
	0.9
	1
Pitch (λ)	0.275
Outerdiameter(Do)	0.241
Insidediameter(Di)	0.123
Turbine length(T_L)	2
Bladenumber(N)	Twoblade

The Archimedes Screw Turbine geometric design was created using SOLIDWORKS software. The model was then exported into ANSYS for the meshing process prior to simulation as shown in Fig. 2.
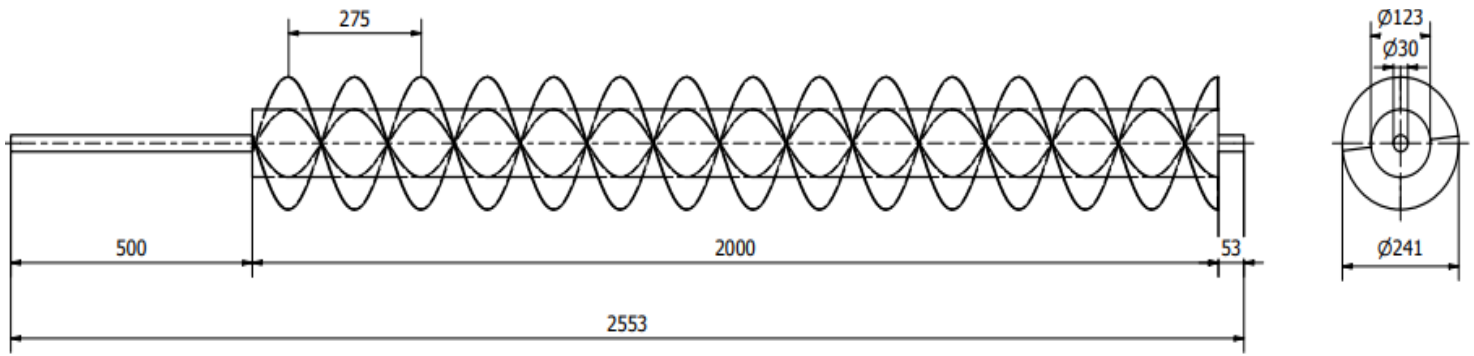
Fig. 1. Archimedes turbine design.
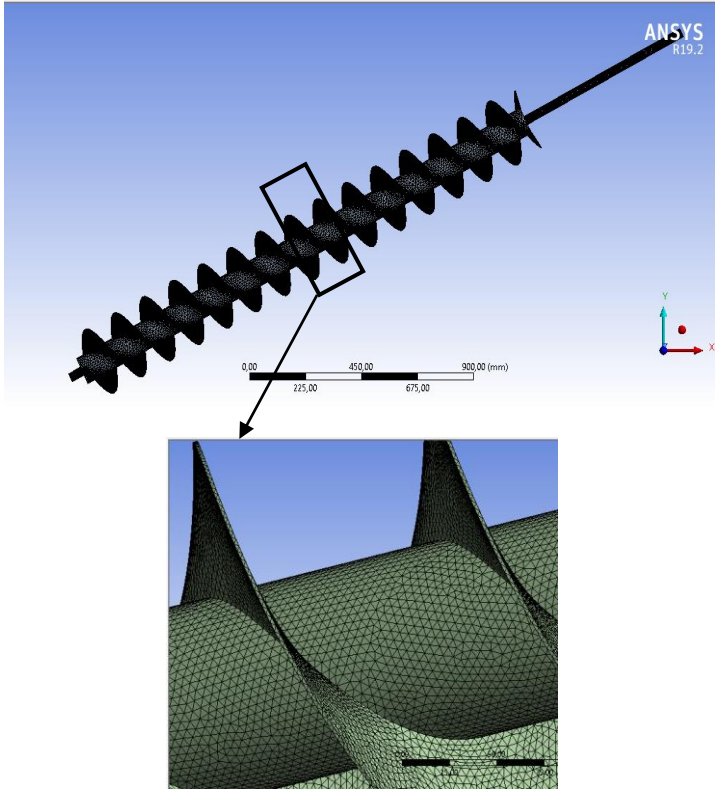
Fig. 2. Meshing model in turbine geometry.
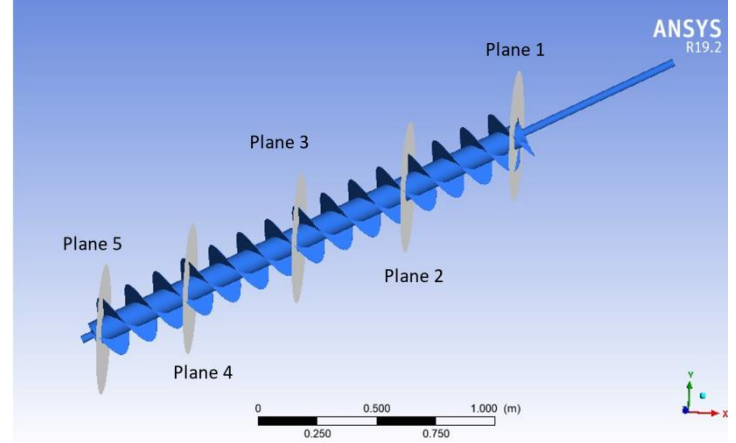
Fig. 3. Location of planes.

The geometric shape determines the choice of mesh type in the modeling process. When dealing with intricate shapes, especially those involving annulus shapes, the tetrahedral mesh type is considered suitable due to its ability to accommodate complex geometries[25].

Data is collected for pressure to assess the flow pattern of energy working along the turbine. The specific locations for scrutinizing the pressure pattern include the turbine inlet, turbine center, and turbine outlet. Fig. 3 illustrates the determination of plane locations, divided into five sections at distances of 0.25 m, 0.7 m, 1 m, 1.6 m, and 2 m from the turbine inlet. This segmentation allows for a comprehensive examination of the flow patterns at different points along the turbine, providing valuable insights into the system's dynamic behavior.

The analysis of fluid flow patterns in the Archimedes screw turbine system relies on input parameters determined by standard values provided by the CFD software, which align with the specific fluid conditions applied. The selection of input data must be tailored to the defined objectives and parameters. The simulation employs the analysis of Partial Differential Equations (PDE) to interpret conservation laws, encompassing mass, momentum, and energy, transforming them into numerical formulations. Conservation laws play a pivotal role in solving simulation problems through CFD. According to the fluid mass balance, the rate of change in fluid mass equals the mass flow rate into the fluid section. As fluid properties vary with space (x, y, z) and time (t), the fluid density ρ is expressed as ρ (x, y, z, t), and fluid velocity components are denoted as dx/dt = u, dy/dt = v, and dz/dt = w. The Eq. 1 represents non-compressible fluids under steady conditions [22].

$$\frac{\partial(\rho u)}{\partial x} + \frac{\partial(\rho v)}{\partial y} + \frac{\partial(\rho w)}{\partial z} = 0 \tag{1}$$

where ρ is the fluid density (kg/m^3) and x, y, z are the Cartesian coordinate directions.

The momentum equation was developed from the Navier-Stokes equation using the finite volume method according to the steady state[26] as shown in Eq. 2-Eq. 4.

x-momentum:

$$\left[\frac{\partial(\rho u)}{\partial t} + \frac{\partial(\rho u^2)}{\partial x} + \frac{\partial(\rho uv)}{\partial y} + \frac{\partial(\rho uw)}{\partial z}\right] = -\frac{\partial p}{\partial x} + \frac{1}{Re_f}\left[\frac{\partial \tau_{xx}}{\partial x} + \frac{\partial \tau_{xy}}{\partial y} + \frac{\partial \tau_{xz}}{\partial z}\right] \tag{2}$$

y-momentum:

$$\left[\frac{\partial(\rho u)}{\partial t} + \frac{\partial(\rho u^2)}{\partial x} + \frac{\partial(\rho uv)}{\partial y} + \frac{\partial(\rho uw)}{\partial z}\right] = -\frac{\partial p}{\partial x} + \frac{1}{Re_f}\left[\frac{\partial \tau_{xx}}{\partial x} + \frac{\partial \tau_{xy}}{\partial y} + \frac{\partial \tau_{xz}}{\partial z}\right] \tag{3}$$

z-momentum:

$$\left[\frac{\partial(\rho w)}{\partial t} + \frac{\partial(\rho uw)}{\partial x} + \frac{\partial(\rho vw)}{\partial y} + \frac{\partial(\rho w^2)}{\partial z}\right] = -\frac{\partial p}{\partial z} + \frac{1}{Re_f}\left[\frac{\partial \tau_{xz}}{\partial x} + \frac{\partial \tau_{yz}}{\partial y} + \frac{\partial \tau_{zz}}{\partial z}\right] \tag{4}$$

This equation is resolved through an iterative method. The initial solution value is typically the necessary estimate of to initiate the calculation. Numerical equations generate more precise estimates when all variables align with the three fluid flow equations.

In this study, the k-ε model was used with a turbulence intensity of 5%, due to the turbulent flow conditions in the turbine, which are characterized by fluctuating speeds. Boundary condition at inlet velocity normal to boundary and reference frame wall absolute. The simulation modeling used in this study is decribed in reference [12].

The newly derived value is subsequently employed as the initial value in successive calculations. This process continues until the error value or residual change becomes sufficiently small or converges. Each repetition in the process of attaining a solution is referred to as an iteration. For steady-state analysis, the calculation process is reiterated until convergence. In non-steady-state conditions, the process persists until the subsequent calculation is complete.

3 Results and Discussion

The CFD results-primarily depict the pressure distribution characteristics in the Archimedes turbine. Changes in pressure along the turbine signify the momentum responsible for the turbine's performance. The simulation encompasses two flow discharge variations, $Q_1 = 0.0125$ m^3/s and $Q_2 = 0.025$ m^3/s. The experimental data utilized refers to the research on the experimental study of the effect of flow on Archimedes Screw Turbines [14].

3.1 Pressure Distribution at $Q_1 = 0.0125$ m^3/s

Fig. 4 illustrates the pressure distribution along the turbine. This figure displays the flow patterns within the turbine at various heads. The observed pattern indicates that the inlet is larger than the outlet, attributing this asymmetry to fluid flow collision at the inlet, converting into momentum that drives turbine rotation. This observation aligns with findings from Omar's research [25], which noted a decrease in pressure inside the Archimedes Screw Turbine due to an increase in flow velocity along the turbine. Flow velocity changes lead to kinetic energy variations, transforming into rotational energy. Consequently, closer to the outlet, the static pressure of the flow decreases.
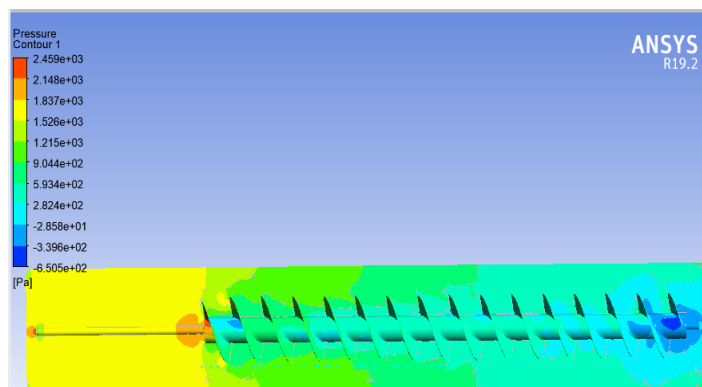
(a)
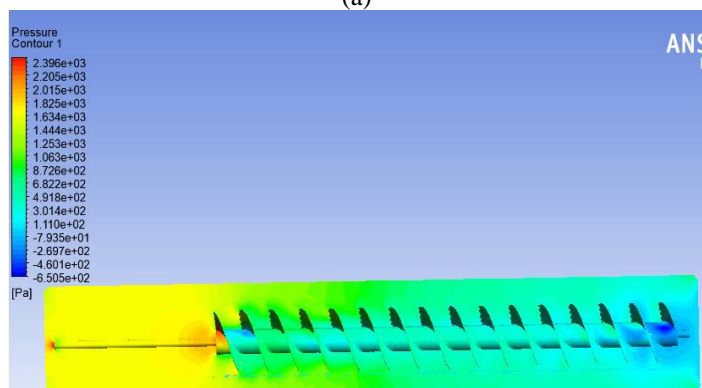
(b)
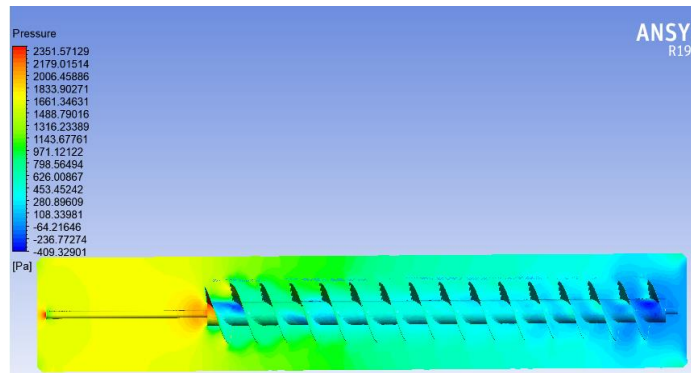
(c)
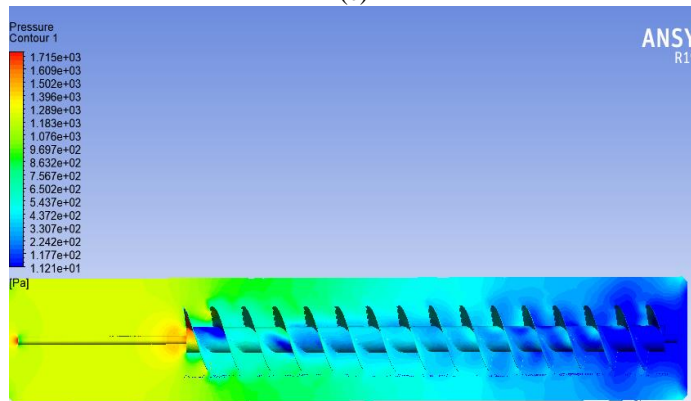
(d)

Fig. 4. Pressure count on the turbine.

At a head of 1 m, the pressure contour changes from the inlet to the outlet, exhibiting a relatively consistent color gradient. Shallow pressure initiates near the outlet, where water flows toward atmospheric pressure. This suggests that at a 1-meter head, the flow maintains pressure until it eventually exits the outlet. Notably, the pressure drop pattern at a 1-meter head is lower than that of turbines with lower heads. A pronounced pressure drop is evident in turbines with a 0.7-meter head, where low pressure encompasses 2/3 of the turbine. This scenario indicates a substantial pressure loss before exiting the turbine, significantly influencing its rotation. After low pressure, the flow lacks kinetic energy, merely passing through the turbine.

The flow pressure pattern highlights that the most significant pressure within the turbine is concentrated at the inlet and diminishes as it progresses toward the outlet for different heads, as illustrated in Fig. 5.
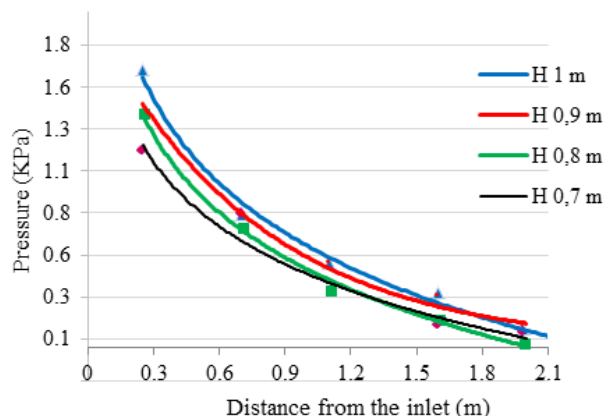
Fig. 5. Pressure distribution pattern in Q_1.

Fig. 5 illustrates the pressure distribution pattern in Q_1. The highest pressure is observed at a 1-meter head, measuring 1,652 KPa, which is significantly larger than that of other heads. The pressure gradually decreases towards the inlet and further diminishes towards the outlet. In contrast, a distinct phenomenon is noted at the outlet of the 0.7-meter turbine head. While following a similar trend to other heads, the pressure at a distance

of 1.5 m from the inlet has decreased to 0.036 kPa. This suggests that the turbine operates optimally at lower flow rates, specifically at a head of 0.8 meters, indicating potential improvements in the turbine performance at smaller heads.

3.2 Pressure Distribution at $Q_2 = 0.025$ m³/s

The pressure distribution pattern in the turbine at a flow rate of 0.025 m³/s is depicted in Figure 6. The pressure pattern at flow rate Q_2 mirrors that at Q_1. However, the pressure drop pattern exhibits slight differences at heads of 0.7 and 0.8 meters. The higher initial speed results in more significant initial momentum, providing more incredible energy to the turbine blade and lowering the pressure drop compared to a lower flow rate.

When entering the turbine, as shown in Figure 7, it can be seen that the highest-pressure value is obtained at a head of 1 m, namely 2.2 KPa. It is much higher than other heads.

This occurs because the impact occurs perpendicular to the turbine blade. A pressure drop occurs as the flow enters the turbine outlet. When entering the outlet, the pressure decreases significantly at each head until it finally reaches atmospheric pressure.

Notably, based on the simulation outcomes, there is a discernible decrease in pressure as the free stream velocity increases. Nevertheless, the maximum flow rate enables the turbine to function effectively at heads lower than 1 meter. The water pattern remains consistent, wherein upon entering the turbine, the pressure reaches its peak at the turbine inlet and diminishes towards the outlet due to the transformation of compressive energy into rotational energy.

(a)

(b)

(c)

(d)
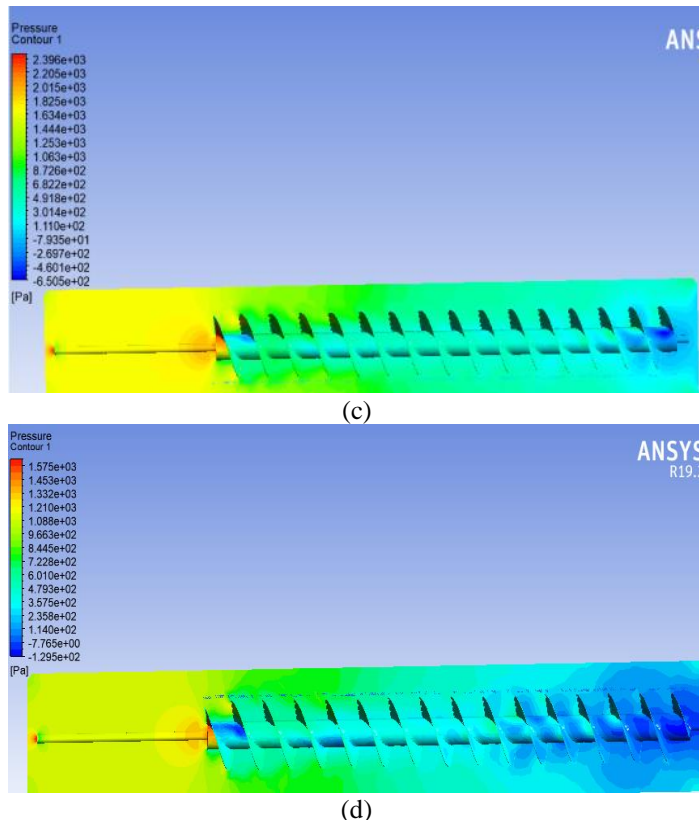
Fig. 6. Pressure contour at flow rate Q_2.

3.3 Comparison Graph of Highest and Lowest Head Pressure

Simulation results for heads of 0.7 and 1 m at flow rates of 0.0125 m³/s and 0.025 m³/s are depicted in Fig. 8. A comparative analysis of the highest and lowest head values under varying flow rates makes the influence of flow rate on the resulting pressure pattern apparent.

The illustration above indicates that the flow rate $Q_2=0.025$ m³/s, denoted by a dotted line, exhibits higher pressure than $Q_1=0.0125$ m³/s. Despite the nearly identical pressure drop pattern, the disparity in pressure values at a head of 1 m and a head of 0.7 m is negligible in Q_2. This suggests that the turbine's performance remains robust at higher flow rates, even with a lower head. The initial flow momentum persists until it approaches the outlet, retaining sufficient energy to rotate the turbine. In contrast, in Q_1, with a smaller flow rate, the difference in head has a significantly more pronounced impact.
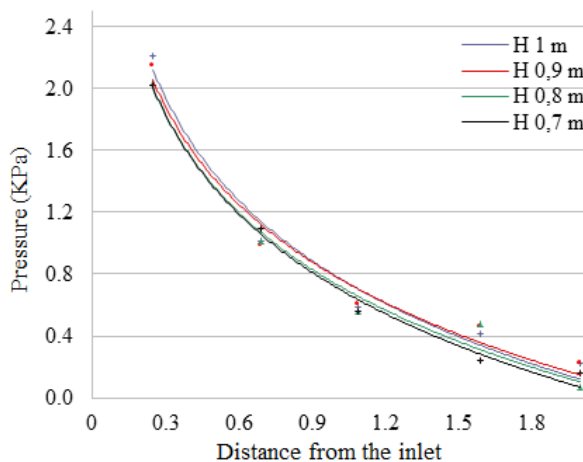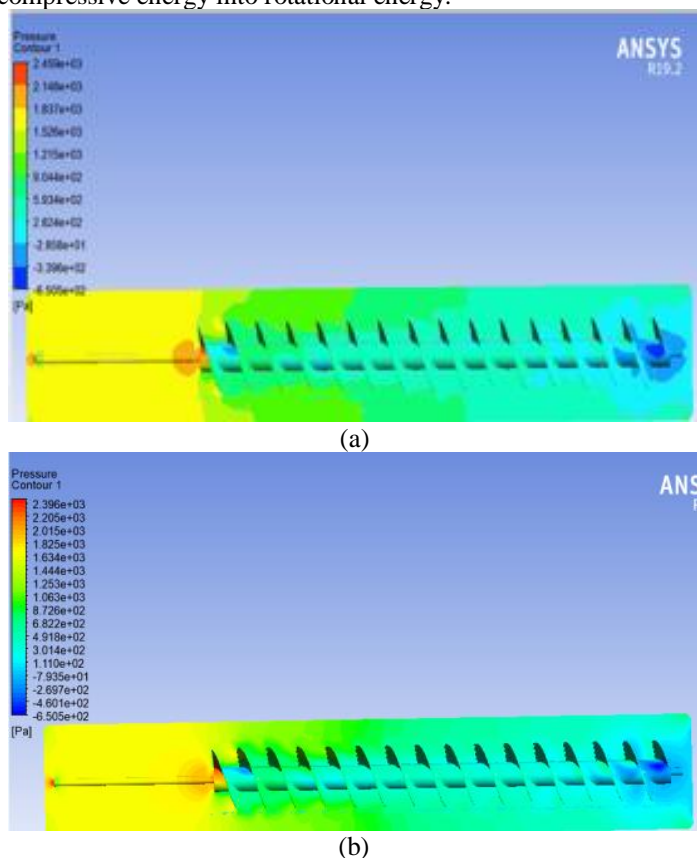
Fig. 7. Pressure distribution pattern in Q_2.
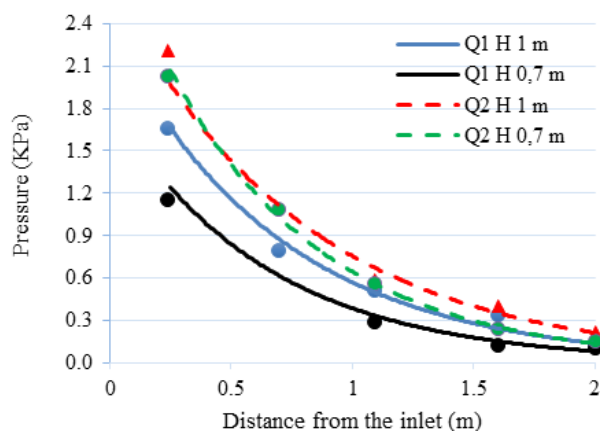
Fig. 8. Pressure distribution comparison.

4 Conclusion

The simulation results obtained through CFD precisely reveal the flow patterns within the turbine and the nuanced pressure gradations along the turbine. A surface pressure distribution simulation on the turbine is conducted by idealizing the flow, directly calculating the pressure to meet design objectives, and observing the pattern of pressure changes.

In conclusion, following simulations across various heads and flow rate variations, it becomes evident that the performance of the Archimedes double-screw turbine is optimized at higher flow rates, specifically at a flow of 0.025m^3/s. Despite the peak performance occurring at a 1-meter head, the observed pressure pattern indicates that the flow retains sufficient energy to rotate the turbine even at a head of up to 0.7 meters.

References

[1] W. Bank, I. Energy Agency, I. Renewable Energy Agency, U. Nations Statistics Division, and W. Health Organization, "A joint report of the custodian agencies THE ENERGY PROGRESS REPORT," 2020. [Online]. Available: www.worldbank.org

[2] IESR, "Indonesia Energy Transition Outlook 2022," *Iesr*, pp. 1–93, 2021.

[3] T. Government, E. B. Plan, N. Electricity, G. Plan, and N. D. Contributions, "RUPTL 2021-30 : PLN steps up ambitions to accelerate clean energy investments in Indonesia," pp. 3–6, 2021.

[4] O. Shofiyah, C. Mutia Gunandar, and Tasha Devi Ariyanti Vincensia, "Efektivitas pembangkit listrik tenaga mikrohidro sebagai penyedia energi baru terbarukan berbasis komunitas," *SEESDGJ*, vol. 1, no. 1, pp. 63–77, 2023, doi: 10.61511/seesdgj.v1.

[5] S. C. Simmons and W. D. Lubitz, "Archimedes screw generators for sustainable micro-hydropower production," *Int. J. Energy Res.*, vol. 45, no. 12, pp. 17480–17501, 2021, doi: 10.1002/er.6893.

[6] A. Dinas Energi dan Sumber Daya Mineral, "Kapasitas Potensi Pembangkit Tenaga Air menurut Pembangkit Listrik tenaga air yang diakumulasikan hingga tahun 2021," 2023.

[7] A. YoosefDoost and W. D. Lubitz, "Archimedes screw turbines: A sustainable development solution for green and renewable energy generation-a review of potential and design procedures," *Sustain.*, vol. 12, no. 18, 2020, doi: 10.3390/SU12187352.

[8] C. Purece and L. Corlan, "Archimedean screw as fish-friendly turbines for harnessing hydropower potential," *E3S Web Conf.*, vol. 286, p. 02007, 2021, doi: 10.1051/e3sconf/202128602007.

[9] A. Y. and H. MI Maulana, "Initial Review and Design of Archimedes Screw Turbine As Low Head Power Station," *Proc. Natl. Conf. Technol. Eng*, no. 7, pp. 111–115, 2015.

[10] C. Rorres, "The Turn of the Screw: Optimal Design of an Archimedes Screw," *J. Hydraul. Eng.*, vol. 126, no. 1, pp. 72–80, 2000, doi: 10.1061/(asce)0733-9429(2000)126:1(72).

[11] M. A. N. Mu'tasim, N. S. Azahari, and A. A. A. Adam, "Prediction of particle impact on an archimedes screw runner blade for micro hydro turbine," *Appl. Mech. Mater.*, vol. 465–466, no. June 2017, pp. 552–556, 2014, doi: 10.4028/www.scientific.net/AMM.465-466.552.

[12] M. I. Maulana, A. Syuhada, and M. Nawawi, "Blade number impact on pressure and performance of Archimedes screw turbine using CFD," *AIP Conf. Proc.*, vol. 1931, no. February 2018, 2018, doi: 10.1063/1.5024096.

[13] D. M. Nuernbergk and C. Rorres, "Analytical Model for Water Inflow of an Archimedes Screw Used in Hydropower Generation," *J. Hydraul. Eng.*, vol. 139, no. 2, pp. 213–220, 2013, doi: 10.1061/(asce)hy.1943-7900.0000661.

[14] M. I. Maulana, A. Syuhada, and R. Kurniawan, "Experimental study on the effect of flow rate on the performance of two-blade archimedes screw turbine," *J. Adv. Res. Fluid Mech. Therm. Sci.*, vol. 61, no. 1, pp. 10–19, 2019.

[15] G. Dellinger, S. Simmons, W. D. Lubitz, P. A. Garambois, and N. Dellinger, "Effect of slope and number of blades on Archimedes screw generator power output," *Renew. Energy*, vol. 136, pp. 896–908, 2019, doi: 10.1016/j.renene.2019.01.060.

[16] M. I. Maulana, Darwin, and G. S. Putra, "Performance of Single Screw Archimedes Turbine Using Transmission," *IOP Conf. Ser. Mater. Sci. Eng.*, vol. 536, no. 1, 2019, doi: 10.1088/1757-899X/536/1/012022.

[17] N. Adhikari, N. Adhikari, and D. Bastakoti, "Study on Effect of Flow Rate and Number of Blades on Sizing of Archimedes Study on Effect of Flow Rate and Number of Blades on Sizing of Archimedes Screw Turbine," no. July, 2022.

[18] A. T. Ubando, I. A. V. Marfori, M. S. Peradilla, C. L. Sy, A. M. A. Calapatia, and W. H. Chen, "Sustainable Manufacturability of Archimedes Screw Turbines: A Critical Review," *J. Manuf. Mater. Process.*, vol. 6, no. 6, pp. 1–26, 2022, doi: 10.3390/jmmp6060161.

[19] I. Syam, M. I. Maulana, and A. Syuhada, "Design and Performance of Archimedes Single Screw Turbine as Micro Hydro Power Plant with Flow Rate Debit Variations (Case Study in Air Dingin, Samadua - South Aceh)," *J. Inotera*, vol. 4, no. 1, p. 13, 2019, doi: 10.31572/inotera.vol4.iss1.2019.id71.

[20] M. Hasan Basri, A. Muhtadi, and D. Hasan, "Design of a Laboratory Scale Archemedes Screw Turbine Model Hydroelectric Power Station (PLTA) Simulator," *J. Ilm. Tek. Elektro Komput. dan Inform.*, vol. 9, no. 3, pp. 558–570, 2023, doi: 10.26555/jiteki.v9i3.26309.

[21] M. I. Maulana, A. Syuhada, and F. Almas, "Computational fluid dynamic predictions on effects of screw number on performance of single blade Archimedes screw turbine," *E3S Web Conf.*, vol. 67, 2018, doi: 10.1051/e3sconf/20186704027.

[22] G. Dellinger et al., "Computational fluid dynamics modeling for the design of Archimedes Screw Generator," *Renew. Energy*, vol. 118, pp. 847–857, 2018, doi: 10.1016/j.renene.2017.10.093.

[23] K. Shahverdi, "Modeling for prediction of design parameters for micro-hydro Archimedean screw turbines," *Sustain. Energy Technol. Assessments*, vol. 47, p. 101554, Oct. 2021, doi: 10.1016/J.SETA.2021.101554.

[24] K. Shahverdi, R. Loni, J. M. Maestre, and G. Najafi, "CFD numerical simulation of Archimedes screw turbine with power output analysis," *Ocean Eng.*, vol. 231, no. June 2020, p. 108718, 2021, doi: 10.1016/j.oceaneng.2021.108718.

[25] Launder B. E. and S. D. B., "MAN - ANSYS Fluent User' s Guide Releasde 15.0," *Knowl. Creat. Diffus. Util.*, vol. 15317, no. November, pp. 724–746, 2013.

[26] B. Darmono and H. Pranoto, "Archimedes Screw Turbines (ASTs) Performance Analysis using CFD Software Based on Variation of Blades Distance and Thread Number on The Pico Hydro Powerplant," *Int. J. Adv. Technol. Mech. Mechatronics Mater.*, vol. 3, no. 1, pp. 18–25, 2022, doi: 10.37869/ijatec.v3i1.53.